High-temperature electronic devices enabled by hBN-encapsulated graphene

Šiškins, Makars; Mullan, Ciaran; Son, Seok Kyun; Yin, Jun; Watanabe, Kenji; Taniguchi, Takashi; Ghazaryan, Davit; Novoselov, Kostya S.; Mishchenko, Artem

DOI
10.1063/1.5088587

Publication date
2019

Document Version
Final published version

Published in
Applied Physics Letters

Applied Physics Letters

High-temperature electronic devices enabled by hBN-encapsulated graphene

Cite as: Appl. Phys. Lett. **114**, 123104 (2019); https://doi.org/10.1063/1.5088587
Submitted: 11 January 2019 . Accepted: 13 March 2019 . Published Online: 28 March 2019

Makars Šiškins, Ciaran Mullan, Seok-Kyun Son, Jun Yin, Kenji Watanabe, Takashi Taniguchi, Davit Ghazaryan, Kostya S. Novoselov, and Artem Mishchenko

Applied Physics Letters ARTICLE scitation.org/journal/apl

High-temperature electronic devices enabled by hBN-encapsulated graphene

Cite as: Appl. Phys. Lett. **114**, 123104 (2019); doi: 10.1063/1.5088587
Submitted: 11 January 2019 · Accepted: 13 March 2019 ·
Published Online: 28 March 2019

Makars Šiškins,[1,a),b)] Ciaran Mullan,[1,a)] Seok-Kyun Son,[2,c)] Jun Yin,[1] Kenji Watanabe,[3] Takashi Taniguchi,[3] Davit Ghazaryan,[2,4] Kostya S. Novoselov,[1,2] and Artem Mishchenko[1,2,d)]

AFFILIATIONS

[1]School of Physics and Astronomy, University of Manchester, Manchester M13 9PL, United Kingdom
[2]National Graphene Institute, University of Manchester, Manchester M13 9PL, United Kingdom
[3]National Institute for Materials Science, 1-1 Namiki, Tsukuba 305-0044, Japan
[4]Department of Physics, National Research University Higher School of Economics, Staraya Basmannaya 21/4, Moscow 105066, Russian Federation

[a)]**Contributions:** M. Šiškins and C. Mullan contributed equally to this work.
[b)]**Also at:** Kavli Institute of Nanoscience, Delft University of Technology, Lorentzweg 1, 2628 CJ Delft, The Netherlands
[c)]**Also at:** Department of Physics, Mokpo National University, Muan, Jeollanam-do 58554, Republic of Korea
[d)]**Electronic mail:** artem.mishchenko@gmail.com

ABSTRACT

Numerous applications call for electronics capable of operation at high temperatures where conventional Si-based electrical devices fail. In this work, we show that graphene-based devices are capable of performing in an extended temperature range up to 500 °C without noticeable thermally induced degradation when encapsulated by hexagonal boron nitride (hBN). The performance of these devices near the neutrality point is dominated by thermal excitations at elevated temperatures. Non-linearity pronounced in electric field-mediated resistance of the aligned graphene/hBN allowed us to realize heterodyne signal mixing at temperatures comparable to that of the Venus atmosphere (~460 °C).

A growing demand for high-tech devices in applications ranging from oil industry and geological research to aerospace engineering and missions to Venus are generating needs for compact high-temperature electronics and sensors capable of stable operation in extreme environments. Nowadays, most of the standard commercially available electronics fail to operate above 260 °C due to increased leakage currents, decreased dielectric breakdown strength, irreversible thermal damage, etc.[1] As an alternative, the concept of graphene and hexagonal boron nitride (hBN) van der Waals heterostructures provides a method of layer-by-layer engineering of electrical devices out of two-dimensional (2D) materials with atomic precision.[2,3] Considering its outstanding electrical[4,5] and mechanical properties,[6] graphene has potential to become an excellent material for next-generation electronics, while hBN encapsulation guarantees high device quality[7,8] and provides good chemical protection from the environment.[9–11] Calculations predict a phenomenal stability of graphene with a melting point above 4500 K,[12] while recent experimental evidence already suggests a capability of Joule self-heating hBN-encapsulated graphene filaments to operate well above 2000 K.[13–15] Provided that such systems could be adapted to use in high temperatures,[16] they have potential to become a competitor to recently developed Silicon Carbide (SiC) based electronics, which were shown to have the capability of operation at ~460 °C.[17]

In this work, we show that graphene-based electronics can operate at temperatures up to 500 °C by a complete encapsulation in protective layers of hBN. We investigated the operation of both field effect transistors (FETs) and capacitors based on hBN/graphene/hBN heterostructures. A FET device with crystallographic alignment between graphene and hBN was also examined for potential application as a high temperature heterodyne frequency mixer.

In order to access a high temperature regime, we assembled a furnace with a local resistive Joule heater inside a vacuum chamber, where most of the measurements were performed. Using a turbomolecular pumping station, we kept vacuum below 10^{-5} mbar during measurements. The temperature was measured with a resistive temperature detector (PT1000) fixed in the proximity of a sample and controlled through the PID feedback loop. Using a standard dry-transfer procedure of mechanically exfoliated flakes,[8,18,19] we fabricated a device with a single-layer graphene encapsulated within two flakes of hBN on a quartz substrate. A few-layer graphene (FLG) flake

was used as a bottom gate to locally tune the carrier density of single-layer graphene. As shown in Fig. 1(a), the leakage tunnelling current through the bottom hBN reaches 1 nA with 0.53 V/nm at 23 °C and 0.07 V/nm at 400 °C (assuming a minor out-of-plane thermal expansion of hBN[20]). Although the direct tunnelling becomes prominent at excessive gate voltage, V_g, the conductive properties of the graphene channel are not disturbed by minor leakage currents near the charge-neutrality point of graphene. Zero gate voltage tunnelling conductance roughly follows Arrhenius dependence with the activation energy of the order of 0.1 eV. This energy is much lower than the expected height of the graphene/hBN tunnelling barrier (around 1.5 eV, as from Ref. 21) and is probably related to thermal activation of defect-induced transport across the hBN interface.

We observed an unobstructed modulation of the channel resistance, R_{ch}, up to 400 °C [Fig. 1(b)]. To demonstrate that graphene was not degraded throughout multiple heating cycles, we performed detailed Raman spectroscopy of the device before and after the operation at 400 °C. The Raman map was taken across the area of the device. As shown in Fig. 1(c), the full width at half maximum (FWHM) of the 2D peak of graphene has increased in a region above the bottom gate. This effect can be attributed to the increasing contribution of the Raman signal arising from the bottom FLG,[22] since the geometry of the affected region follows that of the underlying flake [see the inset of Fig. 1(a)]. Away from this region, there was no significant change in FWHM of the 2D peak of graphene indicating that no mechanical stress was introduced after the thermal treatment with only minor differences in strain[23] across the device present as FWHM varies at $\pm 2\,\mathrm{cm}^{-1}$. We also show typical Raman spectra obtained away from the proximity of the bottom gate in Fig. 1(d) before and after the thermal cycles. There is no significant change in the normalized intensity, FWHM, or positions of graphene-related peaks, indicating that no notable thermal damage introduced in the hBN encapsulated single-layer graphene flake.

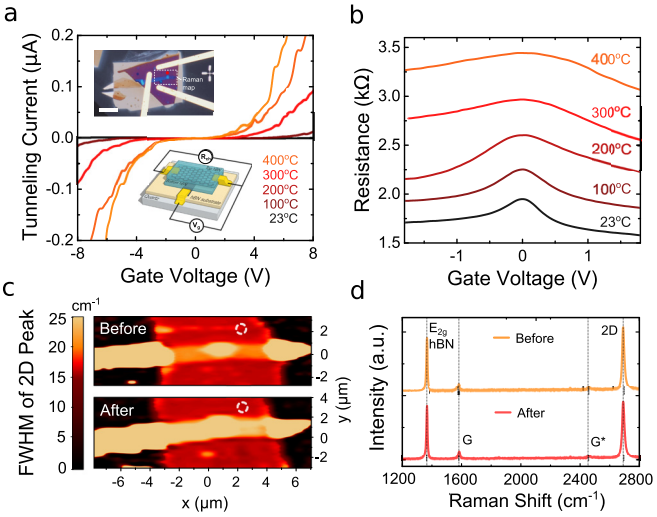

FIG. 1. Transport properties of a single layer graphene field effect transistor at high temperatures. (a) Tunnelling leakage current between graphene and few layer graphene bottom gate at different temperatures. The top inset shows the optical image of the device. Scale bar: 10 μm. The bottom inset shows the schematics of the device. (b) Two-terminal resistance of graphene as a function of gate voltage at different temperatures. (c) Raman maps of the full width half maximum (FWHM) of the 2D peak in the proximity of the gated region. Top and bottom panels were measured before and after multiple thermal cycles up to 400 °C. (d) Raman spectra measured before and after multiple thermal cycles taken at the spot indicated with the dashed white circle in (c).

Most of our high-temperature measurements were performed in a vacuum. For experiments performed in air, we found that performance was similar to that measured in vacuum, up to 450 °C. We noticed, however, an increased device resistance and a shift of the neutrality (Dirac) point suggesting the introduction of inadvertent doping and deterioration of contacts. Comparing these observations with the results of high-current electronic transport in graphene/hBN heterostructures[13–15] (where devices were at high temperatures, but graphene/metal contacts were at ambient temperatures due to efficient thermal dissipation), one can suggest that graphene/metal contacts affect the device performance in an oxidising environment at high temperatures. Although hBN encapsulation is very robust both in a vacuum and in the air, finding suitable electrical contacts would require further studies.

On average, samples were subjected to three thermal cycles from room temperature to 500 °C, with 4–5 h on average above room temperature, 1.5 h above 200 °C, and 0.2–0.5 h above 400 °C (excluding time used to change temperatures). Time spent at temperatures above 400 °C was limited by the overheating of the vacuum setup. We did not observe any deterioration of the sample performance after thermal cycling in a vacuum—in contrast to our observation in ambient conditions.

Thermally induced broadening of the resistance peak at the neutrality point and increase in a general profile of resistance due to the increase in contact resistance noticeably decrease two-point conductance of graphene, $G = 1/R$ with temperature, as indicated in Fig. 1(b). This, nevertheless, shall not be mistaken for a decrease in graphene sheet conductivity, σ_{sheet}. In fact, a gradual smearing of the Dirac peak at $V_g \sim 0$ suggests that the minimum of conductivity of graphene, σ_{sheet}, near the charge neutrality point is limited by increasing the base-level of thermally excited charge carriers[24] in the system, $n_{min}(T)$. To quantitatively study this effect, we fabricated a hBN/graphene/hBN based parallel-plate capacitor within which the single-layer graphene serves as one plate and another gold pad deposited on top of hBN serves as the other plate [see the inset of Figs. 2(a) and 2(b)]. The capacitance between these two plates was measured by a room temperature bridge (AH2700 model). Since single-layer graphene has a low carrier density close to the neutrality point, it manifests as quantum capacitance,[25] C_Q, in series with a geometric capacitance, C_{Geom}, thus, modifying the total capacitance of the device [see Fig. 2(a)]

$$C_D^{-1} = C_Q^{-1} + C_{Geom}^{-1}. \quad (1)$$

The quantum capacitance is directly related to the density of states, D in graphene, $C_Q = e^2 D$, so that the dependence of quantum capacitance on $E_F(V_g)$ can be deduced. For pristine graphene chemical potential, μ can be taken as $\mu = E_F = \hbar \nu_F \sqrt{\pi n}$, where ν_F is the Fermi velocity. The $C_Q - \mu$ curves presented in Fig. 2(b) show that the C_Q plateau forms in the proximity of $\mu = E_F \sim 0$, which is not predicted by the simple model of quantum capacitance for a perfect undoped monolayer graphene and is attributed to the coexistence of thermally excited electrons and holes.[26] We extracted the values of a minimal

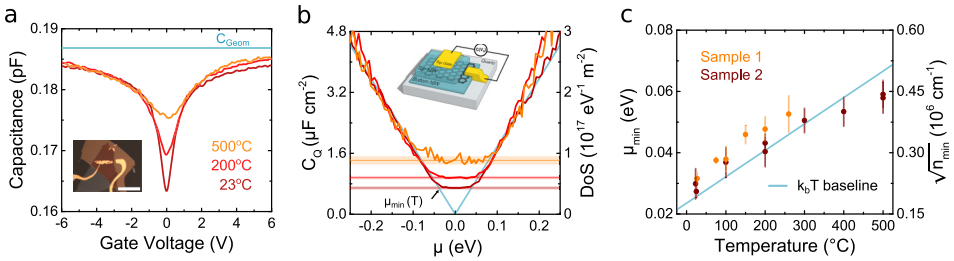

FIG. 2. Thermal effects on the capacitive properties of graphene. (a) Capacitance as a function of gate voltage at different temperatures. The inset shows the optical image of the device. Scale bar: 40 μm. (b) Quantum capacitance as a function of chemical potential at different temperatures. The inset shows the schematics of the device. (c) The minimal charge carrier density level as a function of temperature.

charge carrier density level, $n_{min}(T)$ from the C_Q plateau baseline, and calculated the corresponding chemical potential $\mu_{min}(T) \propto \sqrt{n_{min}(T)}$. As shown in Fig. 2(c), the calculated values follow $k_B T \approx |\mu_{min}(T)|$, which indicates that thermally excited charge carriers dominate the transport properties of graphene near the charge neutrality point at high-temperatures, producing a similar effect to what was observed at cryogenic temperatures but due to electron-hole inhomogeneity caused by the substrate.[26,27]

We took one step further in assessing the thermally influenced performance and stability of hBN/graphene/hBN heterostructures by studying a FET device with graphene aligned to one of the hBN flakes. Lattice parameters of graphene and hBN are different by only ~1.8%, making it a perfect system for studying the superlattice.[28,29] The superlattice potential leads to a significant alteration of the band spectrum of graphene and thus the formation of secondary Dirac points (SDPs) at sub-energies

$$E_{SDP} = \frac{2\pi\hbar v_F}{\sqrt{3}\lambda_M(\theta,\epsilon)}, \tag{2}$$

where $\lambda_M(\theta, \epsilon)$ is the wavelength of the moiré pattern forming on the graphene/hBN interface at a certain angle, θ. The moiré wavelength is highly sensitive to changes in the alignment angle,[28,30] θ, and strain, ϵ, across the sample,[31,32] making an observation of SDPs a sensitive probe for any mechanical effects produced by a thermal treatment. We made an aligned hBN/graphene/hBN device and examined the evolution of SDPs in quantum capacitance approaching from 0.3 K to 380 K. Figure 3(a) shows a number of minor SDPs appearing at sub-energies, which can be attributed to the inhomogeneity of strain across the sample[31,32] or the second-order modification of the graphene electron structure by the top hBN flake.[33] The capacitance spectrum is dominated by the most pronounced sharp peak at $E_{SDP} = \pm 0.196$ eV, indicating a nearly perfect alignment between graphene and hBN, i.e., $\lambda_M \approx 13.9$ nm and $\theta \approx 0°$. In capacitance measurements at high temperatures, the SDP smears out due to thermal excitations. The SDPs, however, were found to be more pronounced in the two-probe resistance of graphene at >100 °C. We assessed the transconductive properties of the device up to 300 °C. Figure 3(b) shows that the SDPs significantly broaden with increasing temperature for both positive and negative applied gate voltages, V_g, but yet remain observable in the whole tested temperature range.

The aligned FET device has a significantly non-linear response with respect to the applied gate voltage, V_g. This is a characteristic feature of the electronic structure of the aligned graphene/hBN heterostructure, which remains dominant up to extremes of the studied temperature range, as can be noted from Fig. 3(b). This non-linearity endows graphene with potential applications in signal processing and modulation techniques, such as heterodyne frequency mixing.[34]

A heterodyne mixer is used to create new frequencies by mixing two signals of certain frequency, $f_{1,2}$, and has wide applications in the wireless communication area. The output of such an operation would produce two distinct signals on frequencies of $f_1 \pm f_2$. During our

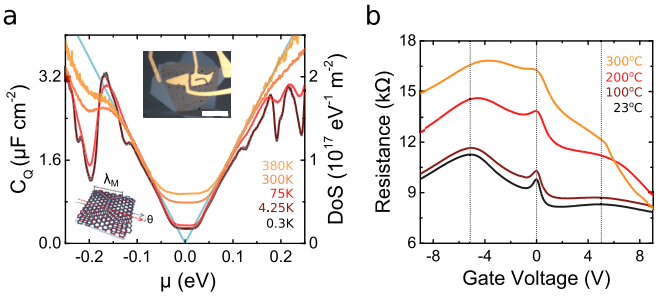

FIG. 3. Thermal effects on the capacitive and transport properties of graphene/hBN superlattices. (a) Quantum capacitance spectrum of the aligned device. Inset—optical image of the device and schematic of the graphene/hBN moiré pattern. Scale bar: 40 μm. (b) Two-terminal resistance of an aligned graphene/hBN FET device.

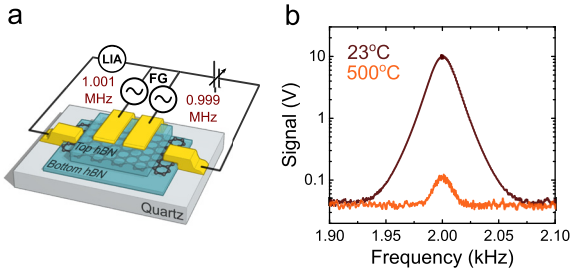

FIG. 4. Heterodyne frequency mixing. (a) Schematics of the device and measurement circuit. (b) The output signal at heterodyne frequency ($f_1 - f_2$) measured at 23 °C and 500 °C.

prototype tests, we applied 5 V peak-to-peak AC signals to both gates of the device, as indicated in Fig. 4(a), with $f_1 = 1.001$ MHz and $f_2 = 0.999$ MHz, respectively. A signal with a frequency of 2 kHz was clearly distinguishable at both 23 °C and 500 °C [Fig. 4(b)], although the signal-to-noise ratio (SNR) reduces from ~674 at room temperature to ~7 at 500 °C. Nevertheless, this is the first demonstration of capabilities of graphene used as a heterodyne mixer even at high temperature. We did not observe any declines in the performance of our frequency mixer up to ~1 MHz limited by the equipment we used. From the channel resistance and parasitic cable capacitance, we estimate that the cut-off frequency should be in the range of 5–10 MHz, which can be substantially improved by the careful design of the transmission lines.

In conclusion, we demonstrated that devices based on hBN/graphene/hBN heterostructures are capable of operation in a high temperature range. No notable degradation of the device properties was observed with temperature up to 500 °C, higher than the temperature of the Venus atmosphere. The transport behaviour of graphene at elevated temperatures was dominated by thermal excitations, especially close to the neutrality point, giving rise to a plateau in the capacitive spectrum. The non-linearity resulting from the recursive energy spectrum of aligned graphene/hBN superlattices makes graphene appropriate for application as a heterodyne frequency mixer. We believe these could open up perspectives for potential use of graphene/hBN electronics for space missions and satellite applications.

This work was supported by the European Research Council, the EU Graphene Flagship Program, the Royal Society, the Air Force Office of Scientific Research, the Office of Naval Research, and the ERC Synergy Grant Hetero2D. Artem Mishchenko acknowledges the support of the EPSRC Early Career Fellowship EP/N007131/1. The authors are grateful to Mark C. Sellers for his help in building the high-temperature setup.

REFERENCES

[1]J. Watson and G. Castro, "A review of high-temperature electronics technology and applications," J. Mater. Sci.: Mater. Electron. **26**, 9226–9235 (2015).
[2]A. K. Geim and I. V. Grigorieva, "Van der waals heterostructures," Nature **499**, 419–425 (2013).
[3]K. S. Novoselov, A. Mishchenko, A. Carvalho, and A. H. C. Neto, "2D materials and van der waals heterostructures," Science **353**, aac9439 (2016).
[4]K. S. Novoselov, A. K. Geim, S. V. Morozov, D. Jiang, Y. Zhang, S. V. Dubonos, I. V. Grigorieva, and A. A. Firsov, "Electric field effect in atomically thin carbon films," Science **306**, 666–669 (2004).
[5]K. S. Novoselov, A. K. Geim, S. V. Morozov, D. Jiang, M. I. Katsnelson, I. V. Grigorieva, S. V. Dubonos, and A. A. Firsov, "Two-dimensional gas of massless Dirac fermions in graphene," Nature **438**, 197–200 (2005).
[6]C. Lee, X. Wei, J. W. Kysar, and J. Hone, "Measurement of the elastic properties and intrinsic strength of monolayer graphene," Science **321**, 385–388 (2008).
[7]C. R. Dean, A. F. Young, I. Meric, C. Lee, L. Wang, S. Sorgenfrei, K. Watanabe, T. Taniguchi, P. Kim, K. L. Shepard, and J. Hone, "Boron nitride substrates for high-quality graphene electronics," Nat. Nanotechnol. **5**, 722–726 (2010).
[8]L. Wang, I. Meric, P. Y. Huang, Q. Gao, Y. Gao, H. Tran, T. Taniguchi, K. Watanabe, L. M. Campos, D. A. Muller, J. Guo, P. Kim, J. Hone, K. L. Shepard, and C. R. Dean, "One-dimensional electrical contact to a two-dimensional material," Science **342**, 614–617 (2013).
[9]Z. Liu, Y. Gong, W. Zhou, L. Ma, J. Yu, J. C. Idrobo, J. Jung, A. H. MacDonald, R. Vajtai, J. Lou, and P. M. Ajayan, "Ultrathin high-temperature oxidation-resistant coatings of hexagonal boron nitride," Nat. Commun. **4**, 2541 (2013).
[10]L. Shen, Y. Zhao, Y. Wang, R. Song, Q. Yao, S. Chen, and Y. Chai, "A long-term corrosion barrier with an insulating boron nitride monolayer," J. Mater. Chem. A **4**, 5044–5050 (2016).
[11]M. Yi, Z. Shen, X. Zhao, S. Liang, and L. Liu, "Boron nitride nanosheets as oxygen-atom corrosion protective coatings," Appl. Phys. Lett. **104**, 143101 (2014).
[12]J. H. Los, K. V. Zakharchenko, M. I. Katsnelson, and A. Fasolino, "Melting temperature of graphene," Phys. Rev. B **91**, 045415 (2015).
[13]S.-K. Son, M. Šiškins, C. Mullan, J. Yin, V. G. Kravets, A. Kozikov, S. Ozdemir, M. Alhazmi, M. Holwill, K. Watanabe, T. Taniguchi, D. Ghazaryan, K. S. Novoselov, V. I. Fal'ko, and A. Mishchenko, "Graphene hot-electron light bulb: Incandescence from hBN-encapsulated graphene in air," 2D Mater. **5**, 011006 (2017).
[14]Y. D. Kim, Y. Gao, R.-J. Shiue, L. Wang, O. B. Aslan, M.-H. Bae, H. Kim, D. Seo, H.-J. Choi, S. H. Kim, A. Nemilentsau, T. Low, C. Tan, D. K. Efetov, T. Taniguchi, K. Watanabe, K. L. Shepard, T. F. Heinz, D. Englund, and J. Hone, "Ultrafast graphene light emitters," Nano Lett. **18**, 934–940 (2018).
[15]H. R. Barnard, E. Zossimova, N. H. Mahlmeister, L. M. Lawton, I. J. Luxmoore, and G. R. Nash, "Boron nitride encapsulated graphene infrared emitters," Appl. Phys. Lett. **108**, 131110 (2016).
[16]Y. Yin, Z. Cheng, L. Wang, K. Jin, and W. Wang, "Graphene, a material for high temperature devices—intrinsic carrier density, carrier drift velocity and lattice energy," Sci. Rep. **4**, 5758 (2014).
[17]P. G. Neudeck, R. D. Meredith, L. Chen, D. J. Spry, L. M. Nakley, and G. W. Hunter, "Prolonged silicon carbide integrated circuit operation in venus surface atmospheric conditions," AIP Adv. **6**, 125119 (2016).
[18]A. Castellanos-Gomez, M. Buscema, R. Molenaar, V. Singh, L. Janssen, H. S. J. van der Zant, and G. A. Steele, "Deterministic transfer of two-dimensional materials by all-dry viscoelastic stamping," 2D Mater. **1**, 011002 (2014).
[19]A. Mishchenko, J. S. Tu, Y. Cao, R. V. Gorbachev, J. R. Wallbank, M. T. Greenaway, V. E. Morozov, S. V. Morozov, M. J. Zhu, S. L. Wong, F. Withers, C. R. Woods, Y.-J. Kim, K. Watanabe, T. Taniguchi, E. E. Vdovin, O. Makarovsky, T. M. Fromhold, V. I. Fal'ko, A. K. Geim, L. Eaves, and K. S. Novoselov, "Twist-controlled resonant tunnelling in graphene/boron nitride/graphene heterostructures," Nat. Nanotechnol. **9**, 808–813 (2014).
[20]W. Paszkowicz, J. Pelka, M. Knapp, T. Szyszko, and S. Podsiadlo, "Lattice parameters and anisotropic thermal expansion of hexagonal boron nitride in the 10-297.5 K temperature range," Appl. Phys. A: Mater. Sci. Process. **75**, 431–435 (2002).
[21]L. Britnell, R. V. Gorbachev, R. Jalil, B. D. Belle, F. Schedin, A. Mishchenko, T. Georgiou, M. I. Katsnelson, L. Eaves, S. V. Morozov, N. M. R. Peres, J. Leist, A. K. Geim, K. S. Novoselov, and L. A. Ponomarenko, "Field-effect tunneling transistor based on vertical graphene heterostructures," Science **335**, 947–950 (2012).
[22]A. C. Ferrari, "Raman spectroscopy of graphene and graphite: Disorder, electron–phonon coupling, doping and nonadiabatic effects," Solid State Commun. **143**, 47–57 (2007).
[23]C. Neumann, S. Reichardt, P. Venezuela, M. Drögeler, L. Banszerus, M. Schmitz, K. Watanabe, T. Taniguchi, F. Mauri, B. Beschoten, S. V. Rotkin, and C. Stampfer, "Raman spectroscopy as probe of nanometre-scale strain variations in graphene," Nat. Commun. **6**, 8429 (2015).
[24]J. Crossno, J. K. Shi, K. Wang, X. Liu, A. Harzheim, A. Lucas, S. Sachdev, P. Kim, T. Taniguchi, K. Watanabe, T. A. Ohki, and K. C. Fong, "Observation of the Dirac fluid and the breakdown of the Wiedemann-Franz law in graphene," Science **351**, 1058–1061 (2016).
[25]S. Luryi, "Quantum capacitance devices," Appl. Phys. Lett. **52**, 501–503 (1988).
[26]H. Xu, Z. Zhang, and L.-M. Peng, "Measurements and microscopic model of quantum capacitance in graphene," Appl. Phys. Lett. **98**, 133122 (2011).
[27]J. Xia, F. Chen, J. Li, and N. Tao, "Measurement of the quantum capacitance of graphene," Nat. Nanotechnol. **4**, 505–509 (2009).
[28]M. Yankowitz, J. Xue, D. Cormode, J. D. Sanchez-Yamagishi, K. Watanabe, T. Taniguchi, P. Jarillo-Herrero, P. Jacquod, and B. J. LeRoy, "Emergence of superlattice Dirac points in graphene on hexagonal boron nitride," Nat. Phys. **8**, 382–386 (2012).
[29]S. Mann, R. Kumar, and V. K. Jindal, "Negative thermal expansion of pure and doped graphene," RSC Adv. **7**, 22378–22387 (2017).
[30]L. A. Ponomarenko, R. V. Gorbachev, G. L. Yu, D. C. Elias, R. Jalil, A. A. Patel, A. Mishchenko, A. S. Mayorov, C. R. Woods, J. R. Wallbank, M. Mucha-Kruczynski, B. A. Piot, M. Potemski, I. V. Grigorieva, K. S. Novoselov, F.

Guinea, V. I. Fal'ko, and A. K. Geim, "Cloning of Dirac fermions in graphene superlattices," Nature **497**, 594–597 (2013).
[31]A. D. Sanctis, J. D. Mehew, S. Alkhalifa, F. Withers, M. F. Craciun, and S. Russo, "Strain-engineering of twist-angle in graphene/hBN superlattice devices," Nano Lett. **18**, 7919–7926 (2018).
[32]D. A. Cosma, J. R. Wallbank, V. Cheianov, and V. I. Fal'ko, "Moiré pattern as a magnifying glass for strain and dislocations in van der Waals heterostructures," Faraday Discuss. **173**, 137–143 (2014).
[33]L. Wang, S. Zihlmann, M.-H. Liu, P. Makk, K. Watanabe, T. Taniguchi, A. Baumgartner, and C. Schönenberger, "New generation of Moiré superlattices in doubly aligned hBN/graphene/hBN heterostructures," Nano Lett. (published online 2019).
[34]Y.-M. Lin, A. Valdes-Garcia, S.-J. Han, D. B. Farmer, I. Meric, Y. Sun, Y. Wu, C. Dimitrakopoulos, A. Grill, P. Avouris, and K. A. Jenkins, "Wafer-scale graphene integrated circuit," Science **332**, 1294–1297 (2011).